BIOCHEMISTRY
including biophysical chemistry & molecular biology

Article

pubs.acs.org/biochemistry

Kinetic Basis for the Differing Response to an Oxidative Lesion by a Replicative and a Lesion Bypass DNA Polymerase from *Sulfolobus solfataricus*

Brian A. Maxwell and Zucai Suo*

Ohio State Biophysics Program and Department of Biochemistry, The Ohio State University, Columbus, Ohio 43210, United States

Supporting Information

ABSTRACT: 8-Oxo-7,8-dihydro-2′-deoxyguanine (8-oxoG), a major oxidative DNA lesion, exhibits ambiguous coding potential and can lead to genomic mutations. Tight control of 8-oxoG bypass during DNA replication is therefore extremely important in hyperthermophiles as the rate of oxidative damage to DNA is significantly increased at high temperatures. Here we employed pre-steady state kinetics to compare the kinetic responses to an 8-oxoG lesion of the main replicative and lesion bypass DNA polymerases of *Sulfolobus solfataricus*, a hyperthermophilic crenarchaeon. Upon encountering 8-oxoG, PolB1, the replicative DNA polymerase, was completely stalled by the lesion, as its 3′ → 5′ exonuclease activity increased significantly and outcompeted its slowed polymerase activity at and near the lesion site. In contrast, our results show that Dpo4, the lone Y-family DNA polymerase in *S. solfataricus*, can faithfully and efficiently incorporate nucleotides opposite 8-oxoG and extend from an 8-oxoG:C base pair with a mechanism similar to that observed for the replication of undamaged DNA. Furthermore, we show that the stalling of PolB1 at the lesion site can be relieved by Dpo4. Finally, the 3′ → 5′ exonuclease activity of PolB1 was the highest when 8-oxoG was mispaired with an incorrect nucleotide and could therefore correct rare mistakes made by Dpo4 during 8-oxoG bypass. These results provide a kinetic basis for a potential polymerase switching mechanism during 8-oxoG bypass whereby Dpo4 can switch with the stalled PolB1 at the replication fork to bypass and extend the damaged DNA and then switch off of the DNA substrate to allow continued replication of undamaged DNA by the more faithful PolB1.

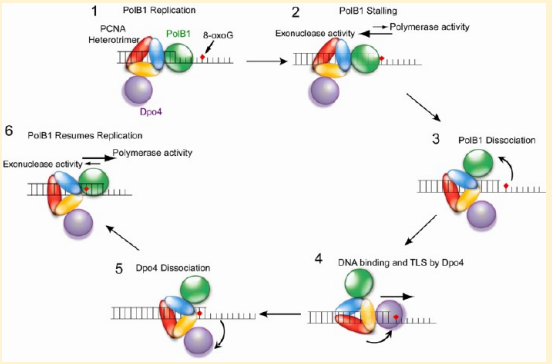

Oxidative damage to cellular DNA can pose significant problems for genomic replication. The reaction of reactive oxygen species with the C8 atom of guanine leads to the formation of 7,8-dihydro-8-oxoguanine (8-oxoG), a very common oxidative DNA lesion.[1,2] This lesion can be highly mutagenic because of its ability to adopt both an *anti* conformation, which forms a correct Watson−Crick base pair with cytosine, and an unusual *syn* conformation, which forms a Hoogsteen base pair with adenine that differs from a canonical T:A pair only minimally in both melting temperature and structure.[3,4] Consequently, DNA polymerases widely differ in their nucleotide incorporation preference opposite an 8-oxoG lesion,[5] with many polymerases favoring misincorporation of dAMP,[6−10] while others preferentially insert correct dCMP opposite 8-oxoG, but with a varying degree of fidelity.[5,7,8,11−16] Structural studies have revealed that nucleotide incorporation preference opposite 8-oxoG depends largely upon how the active site of a DNA polymerase accommodates the additional carbonyl group, which may lead to stabilization of either the *anti* or *syn* conformation of the damaged base.[12,15,17−22] Interestingly, however, recent studies have shown that accessory factor proteins are capable of improving the fidelity of 8-oxoG bypass for several human lesion bypass DNA polymerases.[23,24]

The dual coding potential of 8-oxoG creates difficulties for faithful replication in vivo, especially for hyperthermophiles, such as the crenarchaeon *Sulfolobus solfataricus*, as the incidence of oxidative DNA lesions, including 8-oxoG, is greatly increased at high temperatures.[25] *S. solfataricus* encodes four DNA polymerases,[26] two of which demonstrate a level of polymerase activity insufficient to play a major role in DNA replication.[27] The two remaining, suitably active DNA polymerases include a B-family replicative enzyme, DNA polymerase B1 (PolB1),[26] and a Y-family lesion bypass enzyme, DNA polymerase IV (Dpo4), which is capable of bypassing various DNA lesions.[28−31] PolB1 possesses both DNA polymerase activity and 3′ → 5′ exonuclease activity, while Dpo4 has only the former activity. The fidelity and mechanism of the replication of undamaged DNA catalyzed by both enzymes have been thoroughly investigated in our previously published studies.[32−36] While a full kinetic characterization of the mechanism of 8-oxoG bypass catalyzed by Dpo4 has not been reported, studies have indicated that Dpo4 is capable of preferentially incorporating dCMP over dAMP opposite 8-oxoG because of

Received: February 23, 2012
Revised: March 30, 2012
Published: April 3, 2012

the stabilization of the damaged base in the *anti* conformation through hydrogen bonding between Arg332 in the active site of Dpo4 and the O8 atom of 8-oxoG.[15,20−22] In contrast, data suggest that PolB1 is completely stalled by 8-oxoG,[37] unlike other B-family DNA polymerases that can bypass the lesion with varying degrees of fidelity.[38−40] This suggests that when PolB1 is stalled by 8-oxoG, Dpo4 might take over the replication fork and bypass the lesion to allow genomic replication to continue. This process, termed "polymerase switching", has been suggested to be the general mechanism by which a specialized lesion bypass polymerase is able to rescue stalled replication machinery and perform translesion DNA synthesis (TLS) and then release the primer−template junction to allow continued replication by a higher-fidelity replicative polymerase.[41] *S. solfataricus* represents an attractive model system for investigation of polymerase switching, as there are only two DNA polymerases likely to be involved in the process in vivo. So far, the kinetic basis for polymerase switching in this organism has not been established.

In this study, we performed a thorough pre-steady state kinetic analysis of the response of both Dpo4 and PolB1 to a site-specifically placed 8-oxoG. Our results indicate that, unlike what has been observed for other types of DNA damage,[28,29,31] Dpo4 utilized a mechanism for the bypass and extension of the 8-oxoG lesion similar to the mechanism established for replication of undamaged DNA.[32] Furthermore, we demonstrate that the stalling of PolB1 at the 8-oxoG lesion site stemmed from a sharp increase in its 3′ → 5′ exonuclease activity, rather than the inability of its polymerase activity to incorporate a nucleotide opposite the lesion. Finally, we show that even in the absence of accessory factors, Dpo4 is able to relieve the stalling of PolB1 at the site of DNA damage. Collectively, our studies provide strong insight into how the kinetics of each DNA polymerase can facilitate polymerase switching during TLS of 8-oxoG in *S. solfataricus*.

EXPERIMENTAL PROCEDURES

Preparation of Enzymes and DNA Substrates. Wild-type *S. solfataricus* Dpo4,[33] wild-type PolB1, and the exonuclease-deficient mutant (D231A/E233A/D318A) of PolB1[35] were purified as described previously. The template 30mer containing a site-specifically placed 8-oxoG (Table 1) was purchased from Midland Certified Reagent Co. All other DNA oligomers in Table 1 were purchased from Integrated DNA Technologies, Inc. All oligonucleotides were purified by denaturing polyacrylamide gel electrophoresis (PAGE). For 5′-radiolabeling, the oligonucleotide was reacted with [γ-^{32}P]ATP (MP Biomedicals) in the presence of OptiKinase (USB Corp.) for 3 h at 37 °C. The labeling reaction was then terminated when the mixture was heated at 95 °C for 5 min. The unreacted [γ-^{32}P]ATP was removed using a Bio-Spin 6 column (Bio-Rad Laboratories). Each DNA substrate in Table 1 was annealed as described previously.[33]

Reaction Buffers. All chemical-quench kinetic assays were conducted in buffer R containing 50 mM HEPES, (pH 7.5 at 20 °C), 50 mM NaCl, 0.1 mg/mL BSA, 0.1 mM EDTA, 10% glycerol, and either 5 or 15 mM $MgCl_2$ for Dpo4-catalyzed[33] or PolB1-catalyzed reactions,[35] respectively. Notably, for all assays with PolB1, the enzyme·DNA complex was pre-equilibrated in the absence of $MgCl_2$, which was added upon mixing with dNTP to start reactions. Electrophoretic mobility shift assays were conducted in buffer S containing 50 mM Tris-HCl (pH 7.5 at 20 °C), 50 mM NaCl, 5 mM $MgCl_2$, 0.1 mM EDTA, and 10% glycerol. All reported concentrations indicate the final concentrations upon mixing of all components. All assays were performed at 20 °C.

Table 1. Sequences of DNA Substrates[a]

Name	Sequence
C-16	5′-CGAGCCGTCGCATCCT-3′ 3′-GCTCGGCAGCGTAGGATGGCGGCGTCGTAG-5′
O-16	5′-CGAGCCGTCGCATCCT-3′ 3′-GCTCGGCAGCGTAGGATGGCG**X**CGTCGTAG-5′
O-18	5′-CGAGCCGTCGCATCCTAC-3′ 3′-GCTCGGCAGCGTAGGATGGCG**X**CGTCGTAG-5′
O-19	5′-CGAGCCGTCGCATCCTACC-3′ 3′-GCTCGGCAGCGTAGGATGGCG**X**CGTCGTAG-5′
O-20	5′-CGAGCCGTCGCATCCTACCG-3′ 3′-GCTCGGCAGCGTAGGATGGCG**X**CGTCGTAG-5′
C-21	5′-CGAGCCGTCGCATCCTACCGC-3′ 3′-GCTCGGCAGCGTAGGATGGCGGCGTCGTAG-5′
O-21	5′-CGAGCCGTCGCATCCTACCGC-3′ 3′-GCTCGGCAGCGTAGGATGGCG**X**CGTCGTAG-5′
C-22	5′-CGAGCCGTCGCATCCTACCGCC-3′ 3′-GCTCGGCAGCGTAGGATGGCGGCGTCGTAG-5′
A-22	5′-CGAGCCGTCGCATCCTACCGCA-3′ 3′-GCTCGGCAGCGTAGGATGGCGGCGTCGTAG-5′
O-22	5′-CGAGCCGTCGCATCCTACCGCC-3′ 3′-GCTCGGCAGCGTAGGATGGCG**X**CGTCGTAG-5′
OA-22	5′-CGAGCCGTCGCATCCTACCGCA-3′ 3′-GCTCGGCAGCGTAGGATGGCG**X**CGTCGTAG-5′
O-23	5′-CGAGCCGTCGCATCCTACCGCCG-3′ 3′-GCTCGGCAGCGTAGGATGGCG**X**CGTCGTAG-5′
OA-23	5′-CGAGCCGTCGCATCCTACCGCAG-3′ 3′-GCTCGGCAGCGTAGGATGGCG**X**CGTCGTAG-5′
O-24	5′-CGAGCCGTCGCATCCTACCGCCGC-3′ 3′-GCTCGGCAGCGTAGGATGGCG**X**CGTCGTAG-5′

[a]**X** denotes 8-oxoG.

Electrophoretic Mobility Shift Assays. Increasing concentrations of wild-type Dpo4 (2−256 nM) were added to 5′-^{32}P-labeled DNA (10 nM) and the mixtures allowed to equilibrate for 30 min at 20 °C. The Dpo4·DNA binary complex was separated from free DNA by being run on a 4.5% native acrylamide gel with the running buffer described previously.[28] The dried gel was scanned using a Typhoon Trio (GE Healthcare) and quantitated using ImageQuant (Molecular Dynamics). To determine the K_D^{DNA} for formation of the binary complex, the binary complex concentration was plotted versus the total Dpo4 concentration and the plot was fit to eq 1

$$[\text{E·DNA}] = 0.5(K_D^{DNA} + E_0 + D_0) - 0.5[(K_D^{DNA} + E_0 + D_0)^2 - 4E_0D_0]^{1/2} \quad (1)$$

where E_0 and D_0 are the enzyme and DNA concentrations, respectively.

Pre-Steady State Kinetic Assays. All fast reactions were performed using a rapid chemical-quench flow apparatus (KinTek). For the running start assay, a preincubated solution of a DNA polymerase (100 nM) and 5′-^{32}P-labeled DNA (100 nM) was mixed with a solution containing all four dNTPs (200 μM each) for various times before being quenched with 0.37 M EDTA. The resulting polymerization pattern was resolved by using denaturing PAGE.

To determine the maximal incorporation rate constant (k_p) and apparent equilibrium dissociation constant (K_d) for single-nucleotide incorporation, a preincubated solution of wild-type

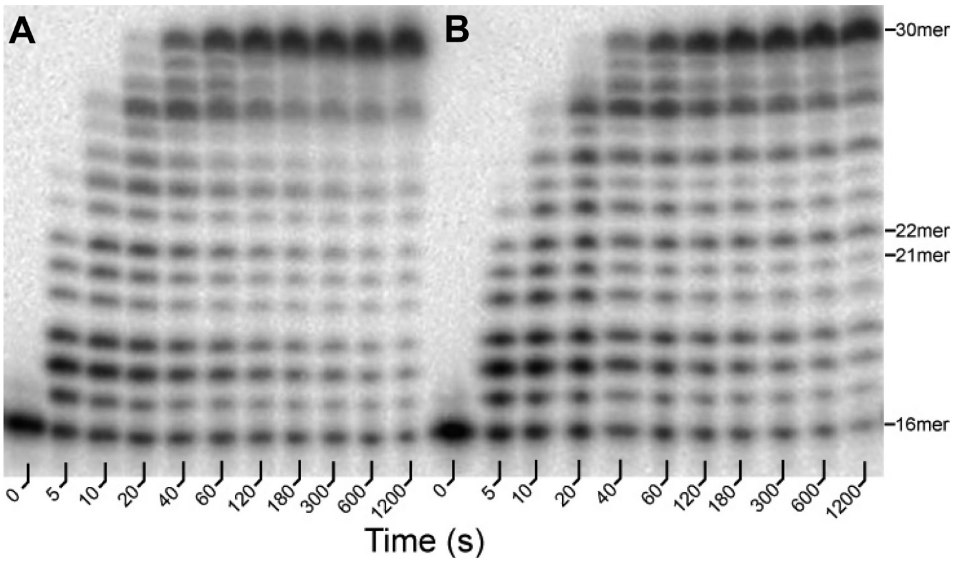

Figure 1. Running start assays with *S. solfataricus* Dpo4 at 20 °C. A preincubated solution of Dpo4 (100 nM) and 5′-^{32}P-labeled DNA (100 nM) was rapidly mixed with a solution containing all four dNTPs (200 μM each), and the reaction was quenched at various times with 0.37 M EDTA. Sizes of the remaining primer and important intermediate products are indicated, and position 22 marks the location of the 8-oxoG lesion from the 3′-terminus of the DNA template: (A) control DNA substrate C-16 and (B) damaged DNA substrate O-16 containing an 8-oxoG lesion (Table 1).

Dpo4 or PolB1 exo− (180 nM) and 5′-^{32}P-labeled DNA (30 nM) was rapidly mixed with increasing concentrations of a single dNTP. For DNA excision assays, wild-type PolB1 (400 nM) was preincubated with DNA (100 nM) and the reaction was initiated with the addition of Mg^{2+} (15 mM). Aliquots of the reaction mixtures were quenched with 0.37 M EDTA at various time intervals. Reaction products were resolved by denaturing PAGE, scanned using a Typhoon Trio (GE Healthcare), and quantitated using ImageQuant (Molecular Dynamics). For each nucleotide concentration, a plot of product concentration versus time was fit to eq 2 using KaleidaGraph (Synergy Software) to obtain an observed rate (k_{obs})

$$[\text{product}] = A[1 - \exp(-k_{obs}t)] \quad (2)$$

where A represents the reaction amplitude. The k_p and apparent K_d values for a single-nucleotide incorporation were then obtained by fitting a plot of the extracted k_{obs} as a function of dNTP concentration to eq 3

$$k_{obs} = k_p[\text{dNTP}]/([\text{dNTP}] + K_d) \quad (3)$$

Data from DNA excision experiments under single-turnover conditions were fit to eq 4

$$[\text{product}] = A \exp(-k_{exo}t) \quad (4)$$

where A and k_{exo} represent the reaction amplitude and observed DNA excision rate, respectively.

For the DNA trap assay, a preincubated solution of Dpo4 (180 nM) and 5′-^{32}P-labeled O-21 or O-22 [30 nM (Table 1)] was mixed rapidly with unlabeled 21/41mer (10 μM) and dCTP or dGTP (1 mM) and the reaction subsequently quenched at various time intervals with 0.37 M EDTA. Data were fit to eq 2.

RESULTS

Bypass of the 8-OxoG Lesion. Previously, strong pause sites characterized by the accumulation of intermediate products opposite to and downstream from DNA lesions have been observed when *S. solfataricus* Dpo4 bypassed an abasic site,[28] cisplatin−d(GpG) adduct,[29,30] or *N*-(deoxyguanosin-8-yl)-1-aminopyrene.[31] To determine if Dpo4 is similarly stalled by a site-specific 8-oxoG, "running start" assays were performed to characterize the extension of DNA substrates O-16 and C-16 (Table 1) in the presence of all four nucleotides. Compared to undamaged C-16 (Figure 1A), Dpo4 efficiently bypassed 8-oxoG in O-16 without significant pausing (Figure 1B), suggesting that the rate of DNA synthesis at and near the lesion site was not affected. In contrast, wild-type PolB1 was almost completely stalled by 8-oxoG (Figure 2B), as observed previously for an abasic site.[28] These results suggest that 8-oxoG represents a legitimate roadblock to DNA replication in *S. solfataricus* and that a switch to Dpo4 may be necessary for the bypass of DNA lesions, including 8-oxoG, in vivo. To determine whether the inability of PolB1 to bypass the lesion was a result of drastically decreased nucleotide incorporation efficiency, we repeated the running start assays with an exonuclease-deficient mutant of PolB1 (PolB1 exo−).[35] Surprisingly, the mutant enzyme was able to bypass the 8-oxoG lesion as demonstrated by the accumulation of the full-length product after 180 s (Figure 2D). However, in contrast to Dpo4, polymerase pausing was observed as indicated by the accumulation of intermediate products at several positions ahead of the lesion site in O-16 (Figure 2D), whereas no enzyme stalling was observed at the corresponding positions in the undamaged C-16 (Figure 2C). Therefore, it is evident that PolB1 exo− was able to incorporate nucleotides adjacent to and opposite the 8-oxoG lesion with a lower efficiency than with undamaged DNA. This finding suggests that the failure of wild-type PolB1 to bypass 8-oxoG likely resulted from increased exonuclease activity in the presence of the lesion, rather than from inhibition of the polymerase activity alone.

In Vitro Polymerase Switching during Lesion Bypass. We next performed running start assays in the presence of both DNA polymerases, to determine if Dpo4 was able to claim the replication fork from a stalled PolB1 and continuously replicate the damaged DNA. When Dpo4 was added to the stalled PolB1

dx.doi.org/10.1021/bi300246r | *Biochemistry* 2012, 51, 3485−3496

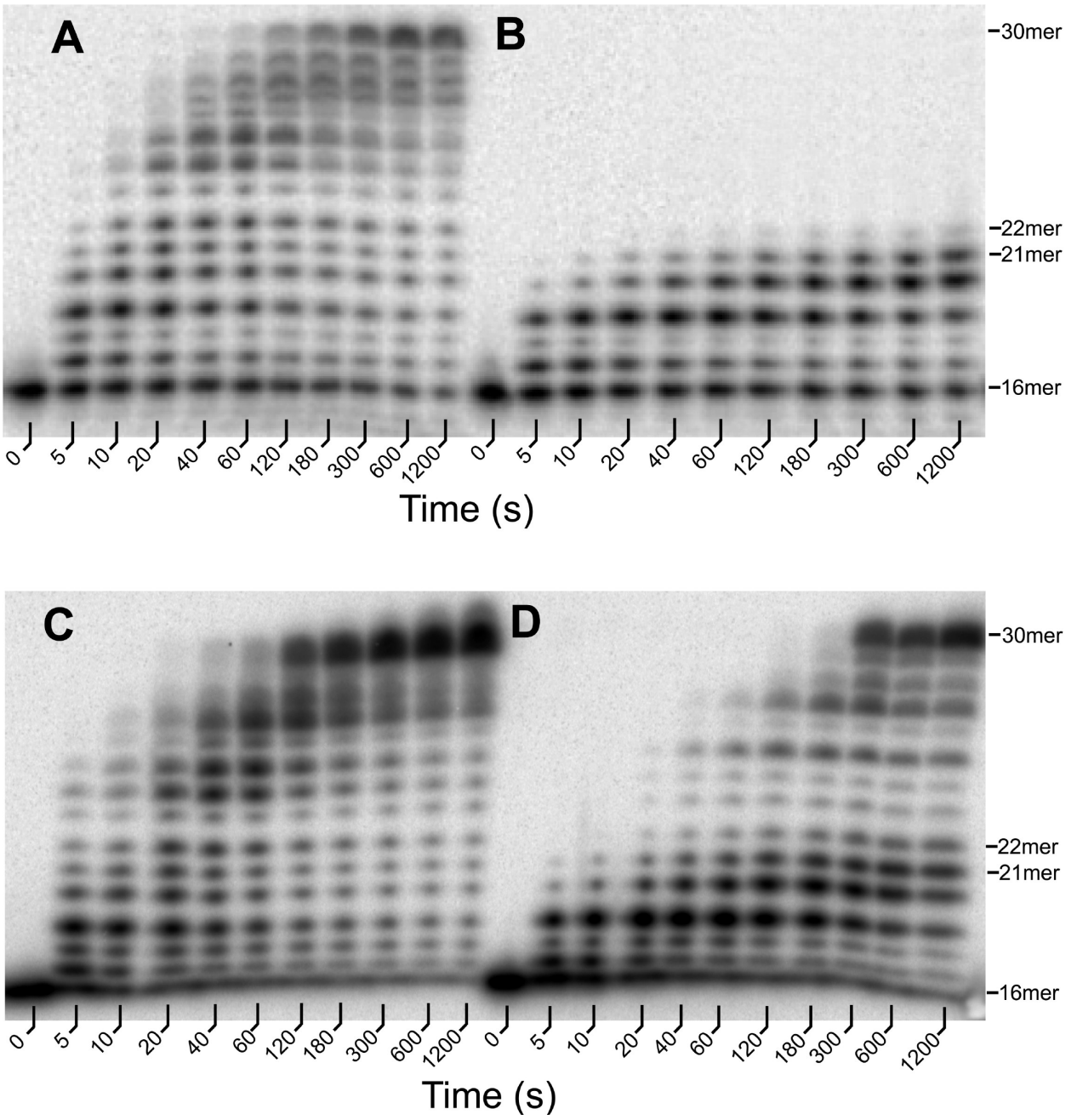

Figure 2. Running start assays with *S. solfataricus* PolB1 at 20 °C. A preincubated solution of PolB1 (100 nM) and 5′-^{32}P-labeled DNA (100 nM) in the absence of Mg^{2+} was rapidly mixed with a solution containing all four dNTPs (200 μM each) and Mg^{2+} (15 mM). The reaction was quenched at various times with 0.37 M EDTA. Sizes of the remaining primer and important intermediate products are indicated, and position 22 marks the location of the 8-oxoG lesion from the 3′-terminus of the DNA template: (A) wild-type PolB1 with control C-16 (Table 1), (B) wild-type PolB1 with damaged O-16 (Table 1), (C) PolB1 exo− with C-16, and (D) PolB1 exo− with O-16.

reaction mixture, both lesion bypass and the subsequent synthesis of full-length products were observed (Figure S1 of the Supporting Information), indicating that Dpo4 was indeed able to exchange with PolB1 to bypass 8-oxoG. Similarly, when a preincubated solution of wild-type PolB1 and O-16 was mixed with a solution containing Dpo4 and all four dNTPs, full-length products were observed after 20 s (Figure 3). Interestingly, some accumulation of 19mer and 20mer was observed, as seen with running start assays in the presence of PolB1 alone (Figure 2B) but not in the same assays with Dpo4 alone (Figure 1). This suggests that PolB1 initially elongated the primer and that Dpo4 likely did not take over replication until position 21 with 8-oxoG as the templating base, where PolB1 alone was stalled (Figure 2B). Notably, similar results were obtained when both Dpo4 and PolB1 were preincubated with DNA prior to mixing with dNTPs (Figure S2 of the Supporting Information), indicating that PolB1 was initially able to outcompete Dpo4 in binding to the DNA substrate before reaching the lesion site. This is consistent with our previous studies that have shown that PolB1 has a 10-fold higher DNA binding affinity than Dpo4.[32,34]

Nucleotide Incorporation and Excision Kinetics of PolB1 in the Presence of the 8-OxoG Lesion. To further investigate the mechanistic details of the stalling of wild-type

dx.doi.org/10.1021/bi300246r | *Biochemistry* 2012, 51, 3485−3496

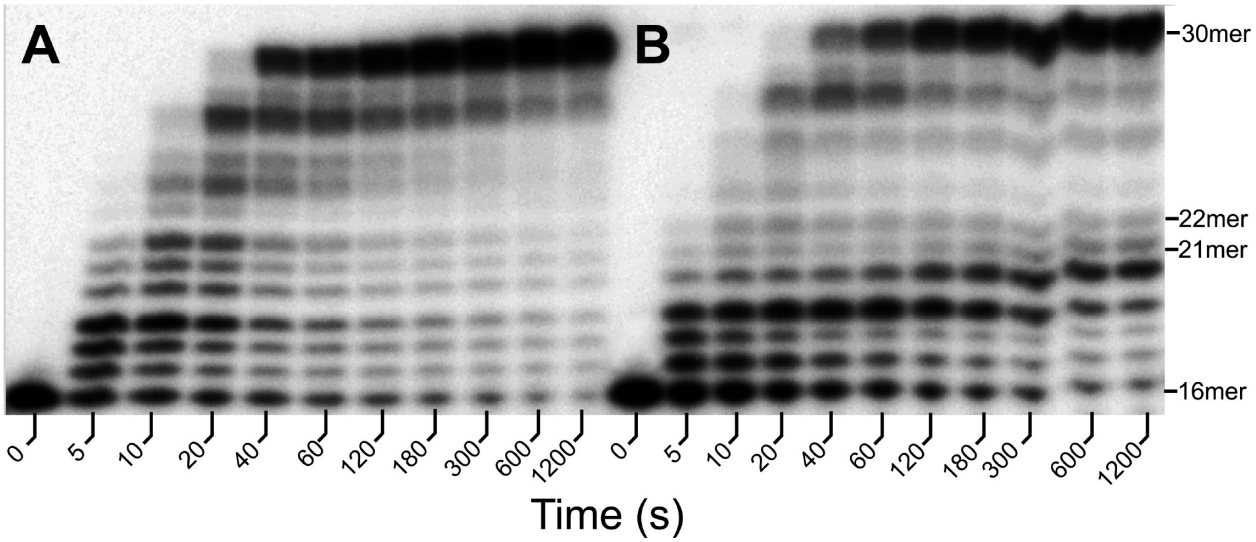

Figure 3. Running start assays with *S. solfataricus* PolB1 and Dpo4 at 20 °C. A preincubated solution of PolB1 (100 nM) and 5′-^{32}P-labeled DNA (100 nM) in the absence of Mg^{2+} was rapidly mixed with a solution containing all four dNTPs (200 μM each), Mg^{2+} (15 mM), and Dpo4 (100 nM). The reaction was quenched at various times with 0.37 M EDTA. Sizes of the remaining primer and important intermediate products are indicated, and position 22 marks the location of the 8-oxoG lesion from the 3′-terminus of the DNA template: (A) control DNA substrate C-16 and (B) damaged DNA substrate O-16 containing an 8-oxoG lesion (Table 1).

PolB1 at the 8-oxoG lesion, we examined the kinetics of nucleotide incorporation and the 3′ → 5′ exonuclease activity in the vicinity of 8-oxoG. As many DNA polymerases exhibit dual coding potential when replicating past 8-oxoG,[5] we performed single-nucleotide incorporation assays to identify the preferred incorporation opposite the lesion. As seen in Figure S3 of the Supporting Information, PolB1 exo− was able to incorporate both correct dCMP and incorrect dAMP opposite 8-oxoG; however, the correct incorporation was more efficient. In comparison, almost no incorporation of incorrect dGMP or dTMP opposite the lesion was observed. Therefore, we preformed single-turnover kinetic analysis to determine the maximal incorporation rate constant (k_p) and apparent nucleotide equilibrium dissociation constant (K_d) of single-nucleotide incorporations to quantitatively compare the incorporation efficiency (k_p/K_d) of dCMP and dAMP opposite both undamaged dG and damaged 8-oxoG (Figure 4). A fit of the plot of the observed incorporation rate (k_{obs}) versus dCTP concentration yielded a k_p of 0.0067 ± 0.0002 s^{-1} and a K_d of 180 ± 20 μM for incorporation of dCMP opposite 8-oxoG (Figure 4B). The efficiency of incorporation of dCMP opposite the lesion was determined to be 3.7×10^{-5} μM^{-1} s^{-1}, 2 orders of magnitude lower than the k_p/K_d measured opposite the undamaged dG, largely because of a 50-fold decrease in k_p (Table 2). The misincorporation of dAMP opposite 8-oxoG was ∼50-fold less efficient than correct dCMP incorporation, indicating that PolB1 exo− is able to faithfully bypass the lesion with a fidelity of 2.1×10^{-2} (Table 2). Additionally, it should be noted that dAMP was incorporated opposite 8-oxoG with a slightly higher efficiency than opposite an unmodified dG, and that both the overall fidelity and correct nucleotide incorporation efficiency of PolB1 exo− are significantly lower with damaged DNA than with undamaged DNA (Table 2).

To examine if the effect of 8-oxoG on the exonuclease activity of PolB1 is the reason behind the polymerase stalling in Figure 2B, we measured the 3′ → 5′ excision rate (k_{exo}) of wild-type PolB1 with damaged and undamaged DNA substrates (Table 1) under single-turnover kinetic conditions (Figure 5 and Figure S4 of the Supporting Information). For substrate O-22 containing a terminal 8-oxoG:C base pair, the k_{exo} was determined to be 0.098 ± 0.009 s^{-1}, nearly 200-fold faster than the rate observed with the corresponding undamaged substrate C-22 and 10-fold faster than with undamaged substrate A-22 containing a terminal G:A mismatch (Table 3). The excision rate was increased even further to 0.28 ± 0.04 s^{-1} in the presence of a terminal 8-oxoG:A base pair in OA-22 (Table 3), indicating that incorporation of either dAMP or dCMP opposite the lesion significantly stimulated the exonuclease activity of wild-type PolB1. Interestingly, compared to that of undamaged DNA, the k_{exo} (Table 3) was also higher with 8-oxoG in the templating position [O-21 (Table 1)] or base-paired with either A or C at position −1 from the primer−template junction [O-23 and OA-23 (Table 1)], but not with 8-oxoG at position −2 (O-24), +2 (O-20), or +3 (O-19). Thus, the exonuclease activity of PolB1 is sensitive to the lesion at the primer−template junction and one position upstream or downstream from the junction, but not at more distant sites (Table 3).

In Figure S5A of the Supporting Information, we determined the k_{obs} for correct nucleotide incorporation at and near the lesion site catalyzed by PolB1 exo− under the same reaction conditions used for the running start experiments (Figure 2). These k_{obs} values and the k_{exo} values measured above (Table 3) establish a kinetic basis for the observed pausing pattern of wild-type PolB1 in Figure 2B (in Scheme 1, forward and reverse reaction rates represent k_{obs} and k_{exo}, respectively). In short, intermediate products accumulated when the rate of product formation (extension of one-nucleotide shorter products and breakdown of one-nucleotide longer products) exceeded the rate of product removal (extension or excision of the product itself). The k_{obs} and k_{exo} values listed in Scheme 1 account for the observed accumulation of 19-, 20-, and 21mer products. Notably, the 21mer → 22mer extension rate (0.0015 s^{-1}) is almost 100-fold lower than the 22mer → 21mer excision rate (0.098 s^{-1}), thus explaining why the intermediate 22mer was barely observed in the running start assay with the wild-

dx.doi.org/10.1021/bi300246r | *Biochemistry* 2012, 51, 3485−3496

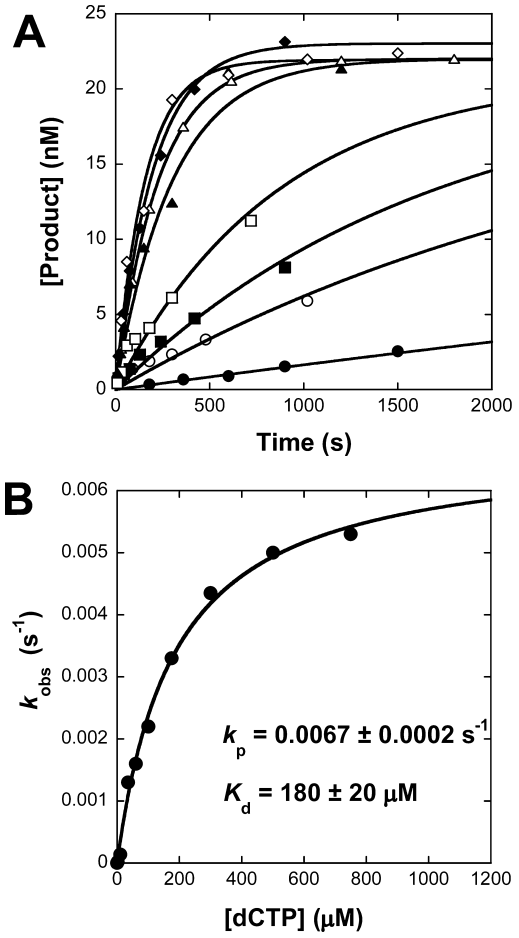

Figure 4. Single-turnover kinetic assays at 20 °C. (A) A preincubated solution of PolB1 exo− (180 nM) and 5′-^{32}P-labeled O-21 (30 nM) was rapidly mixed with increasing concentrations of dCTP [10 (●), 35 (○), 60 (■), 100 (□), 175 (▲), 300 (△), 500 (◆), and 750 μM (◇)] for various time intervals prior to the reaction being quenched with 0.37 M EDTA. Solid lines represent fits to eq 2 to obtain k_{obs}. (B) Plot of k_{obs} vs nucleotide concentration fit to eq 3 to yield the indicated k_p and K_d values.

Table 2. Kinetic Parameters for Incorporation of a Single dNMP into Damaged or Undamaged DNA Substrates (Table 1) at 20 °C Catalyzed by PolB1 exo−

base	k_p (s^{-1})	K_d (μM)	k_p/K_d (μM^{-1} s^{-1})	fidelity[a]
	O-21 (templating base 8-oxoG)			
dC	0.0067 ± 0.0002	180 ± 20	3.7×10^{-5}	
dA	0.0019 ± 0.0001	2400 ± 500	8.0×10^{-7}	2.1×10^{-2}
	C-21 (templating base dG)			
dC	0.36 ± 0.02	70 ± 10	5.1×10^{-3}	
dA	0.00080 ± 0.00009	2600 ± 600	3.1×10^{-7}	6.1×10^{-4}

[a]Calculated as $(k_p/K_{d,incorrect\ dNTP})/(k_p/K_{d,correct\ dNTP} + k_p/K_{d,incorrect\ dNTP})$.

type enzyme (Figure 2). Interestingly, our results show that the negative impact of 8-oxoG on the polymerase and exonuclease activities of PolB1 decreased significantly after the lesion was bypassed. The 23mer → 24mer extension rate (0.21 s^{-1}) and the 24mer → 23mer excision rate (5.4×10^{-4} s^{-1}) are within the error range of the corresponding rates with undamaged DNA (Tables 2 and 3), suggesting that the effect of 8-oxoG disappeared and PolB1 may be able to resume replication after

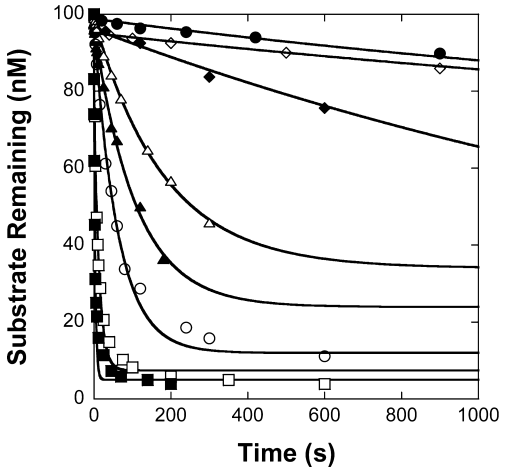

Figure 5. Measurements of 3′ → 5′ exonuclease rates. A preincubated solution of wild-type PolB1 (400 nM) and 5′-^{32}P-labeled DNA (100 nM) was rapidly mixed with Mg^{2+} (15 mM) for varying time intervals prior to the reaction being quenched with 0.37 M EDTA. The concentration of the remaining substrate [O-19 (◆), O-20 (●), O-21 (○), O-22 (□), OA-22 (■), O-23 (△), OA-23 (▲), and O-24 (◇)] was plotted as a function of time. The solid lines represent the fit to eq 4 to yield the DNA excision rates listed in Table 3.

Table 3. The 3′ → 5′ Exonuclease Rates of Wild-Type PolB1 with Damaged and Control DNA Substrates (Table 1) at 20 °C

DNA Substrate	Primer/Template Junction[a]	k_{exo} (s^{-1})
O-19	-C -GCG**X**C-	$(4.3 \pm 0.2) \times 10^{-4}$
O-20	-G -CG**X**C-	$(3.4 \pm 0.6) \times 10^{-4}$
O-21	-GC -CG**X**C-	0.018 ± 0.001
O-22	-GCC -CG**X**C-	0.098 ± 0.009
OA-22	-GCA -CG**X**C-	0.28 ± 0.04
O-23	-GCCG -CG**X**C-	0.0055 ± 0.0004
OA-23	-GCAG -CG**X**C-	0.009 ± 0.001
O-24	-CCGC -G**X**CG-	$(5.4 \pm 0.1) \times 10^{-4}$
C-22	-GCC -CGGC-	$(5.2 \pm 0.2) \times 10^{-4}$
A-22	-GCA -CGGC-	0.0151 ± 0.0006

[a]**X** denotes 8-oxoG.

successful 8-oxoG bypass and the subsequent one-nucleotide extension catalyzed by Dpo4 (see below).

Kinetics of 8-OxoG Bypass Catalyzed by Dpo4. Previous studies have investigated the pre-steady state kinetics of only correct dCMP insertion opposite 8-oxoG.[15] To establish a more complete kinetic basis for 8-oxoG bypass by Dpo4, we performed similar pre-steady state kinetic analysis as described above to determine the k_p and K_d values for all four dNMP incorporations both opposite to and extending from the 8-oxoG lesion (Table 1). The incorporation efficiency (k_p/K_d) of dCMP opposite 8-oxoG in O-21 was determined to be 3.1×10^{-2} μM^{-1} s^{-1} (Figure S6A of the Supporting Information),

dx.doi.org/10.1021/bi300246r | Biochemistry 2012, 51, 3485−3496

Scheme 1

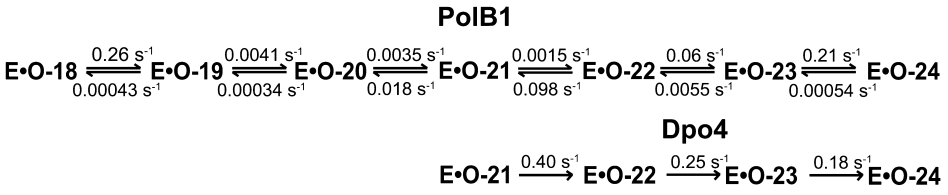

Table 4. Kinetic Parameters for Incorporation of a Single dNMP into Damaged or Control DNA Substrates (Table 1) Catalyzed by Dpo4 at 20 °C

base	k_p (s^{-1})	K_d (μM)	k_p/K_d (μM^{-1} s^{-1})	efficiency ratio[a]	fidelity[b]
		O-21 (templating base 8-oxoG)			
dC	0.43 ± 0.02	14 ± 2	3.1×10^{-2}		
dA	0.22 ± 0.01	929 ± 9	2.4×10^{-4}	1.4×10^{2}	7.2×10^{-3}
dG	0.0011 ± 0.0002	880 ± 90	1.3×10^{-6}	2.5×10^{4}	3.9×10^{-5}
dT	0.026 ± 0.002	800 ± 100	3.3×10^{-5}	1.0×10^{3}	1×10^{-3}
		C-21 (templating base dG)			
dC	0.59 ± 0.02	49 ± 4	1.2×10^{-2}		
dA	0.00126 ± 0.00008	420 ± 80	3.0×10^{-6}	3.7×10^{3}	2.7×10^{-4}
		O-22 (templating base dC, extending from the 8-oxoG:C base pair at position −1)			
dG	0.38 ± 0.01	105 ± 9	3.6×10^{-3}		
dT	0.010 ± 0.002	1900 ± 500	5.3×10^{-6}	6.8×10^{2}	1.5×10^{-3}
dC	0.00072 ± 0.00001	120 ± 10	6.0×10^{-6}	6.0×10^{2}	1.7×10^{-3}
dA	0.0010 ± 0.0001	1000 ± 300	1×10^{-6}	3.6×10^{3}	3×10^{-4}
		C-22 (templating base dC, extending from the G:C base pair at position −1)			
dG	0.38 ± 0.03	290 ± 60	1.2×10^{-3}		

[a]Calculated as $(k_p/K_{d,\text{correct dNTP}})/(k_p/K_{d,\text{incorrect dNTP}})$. [b]Calculated as $(k_p/K_{d,\text{incorrect dNTP}})/(k_p/K_{d,\text{correct dNTP}} + k_p/K_{d,\text{incorrect dNTP}})$.

~3-fold higher than the value of 1.2×10^{-2} μM^{-1} s^{-1} measured for the undamaged substrate C-21 (Table 4). Therefore, unlike that of PolB1, the DNA polymerization activity of Dpo4 was in fact slightly enhanced by the 8-oxoG lesion. In stark contrast, other lesions have been found to decrease correct nucleotide incorporation efficiency by several orders of magnitude and to significantly stall Dpo4 during TLS.[28,29,31] The overall fidelity range for nucleotide incorporation opposite 8-oxoG by Dpo4 (10^{-3} to 10^{-5} in Table 4) is similar to that measured with undamaged DNA (10^{-3} to 10^{-4}).[33,42] Furthermore, dAMP, the most efficient incorrect nucleotide, was incorporated into O-21 with an efficiency 138-fold lower than that of matched dCMP. Thus, Dpo4 can bypass 8-oxoG as faithfully as it replicates undamaged DNA.

As previous studies have shown that lesions are capable of altering the binding of Dpo4 to DNA,[28,29,31] we investigated the effect of the 8-oxoG lesion on the DNA binding properties of Dpo4. Interestingly, 8-oxoG had little effect on the binding affinity of DNA for Dpo4 as suggested by the similarly high binding affinities of O-21 and C-21 estimated through gel mobility shift assays (Figure S7B of the Supporting Information). Furthermore, the binding of O-21 to Dpo4 predominantly formed a productive complex, as with undamaged DNA,[28] demonstrated by the fast monophasic kinetics of incorporation of dCMP into O-21 in the presence of an unlabeled 21/41mer trap DNA (Figure S8 of the Supporting Information). The unlabeled trap DNA serves to effectively sequester any Dpo4 that dissociates from 5′-^{32}P-labeled O-21 (Table 1), thus ensuring that any observed product formation is the result of a single binding event. However, at each Dpo4 pause site with the lesions mentioned above, correct nucleotide incorporation follows biphasic kinetics in the presence of a DNA trap (a small, fast phase precedes a large, slow phase), indicating that the Dpo4·damaged DNA complex exists predominately in a nonproductive conformation.[28,29,31] Together, these kinetic data demonstrate that the conversion of the intermediate product 21mer into a 22mer was slightly facilitated by 8-oxoG and that Dpo4 likely follows the same kinetic mechanism for 8-oxoG bypass as for incorporation of the correct nucleotide into undamaged DNA.[32]

Following lesion bypass, 8-oxoG was embedded in the template and could affect subsequent nucleotide incorporations. As observed with O-21, the 8-oxoG:C base pair had an insignificant effect on the overall binding affinity (Figure S7C of the Supporting Information) and productive binding (Figure S8B of the Supporting Information) of the DNA substrate O-22 (Table 1) to Dpo4. These results, along with the lack of pausing observed in the running start assays (Figure 1B), indicate that the extension after 8-oxoG bypass likely follows the same kinetic mechanism described for undamaged DNA.[32] Unexpectedly, the correct dGMP was incorporated into O-22 (Figure S6B of the Supporting Information) with an efficiency (3.6×10^{-3} μM^{-1} s^{-1}) 3-fold higher than that for incorporation into C-22 (Table 4). Thus, 8-oxoG slightly enhanced the first extension step in addition to 8-oxoG bypass. Notably, the kinetic data with O-21 and O-22 (Table 4) also show that the extension step is ~9-fold less efficient than 8-oxoG bypass; however, this difference was due to DNA sequence dependence, rather than the effect of 8-oxoG, as a similar efficiency ratio was obtained for incorporation of the correct nucleotide into undamaged C-21 and C-22 (Table 4).

DISCUSSION

Despite the low pH and extreme temperature of their natural habitat, in which the rate of DNA damage, including oxidative

dx.doi.org/10.1021/bi300246r | Biochemistry 2012, 51, 3485−3496

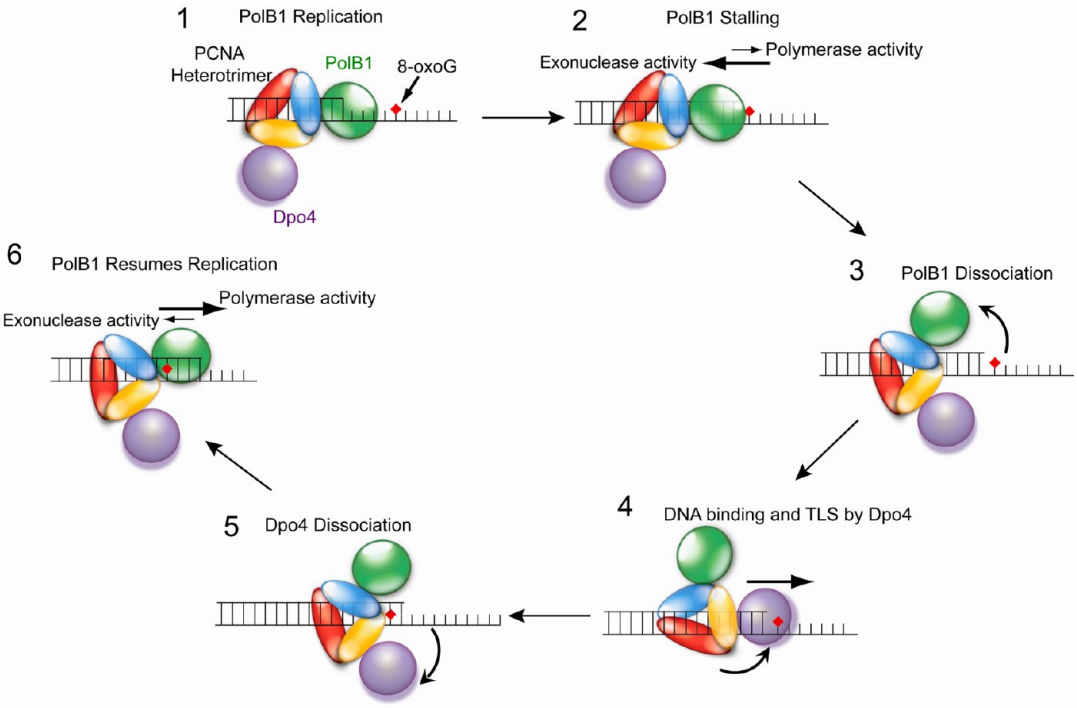

Figure 6. Proposed mechanism for the PCNA-mediated switching between the DNA polymerases of *S. solfataricus* during TLS of 8-oxoG. The sizes of the arrows represent the relative rates of the 3′ → 5′ exonuclease and polymerase activities of PolB1.

damage, is greatly increased,[25] hyperthermophilic Archaea have been shown to achieve lower rates of genomic mutation than mesophilic organisms.[43] To maintain its high genomic stability under such adverse environmental conditions, *S. solfataricus* must utilize an effective system for the efficient and faithful bypass of mutagenic lesions, such as 8-oxoG. Our detailed pre-steady state kinetic analysis has revealed that *S. solfataricus* is able to avoid the difficulties associated with the mutagenic potential of 8-oxoG through the inherited incapability of its replicative DNA polymerase, PolB1, to bypass the lesion. This ensures that during DNA replication the lesion can be bypassed efficiently only after a switch to the lone Y-family polymerase in *S. solfataricus*, Dpo4, which exhibits a fidelity of 8-oxoG bypass among the highest of any DNA polymerase characterized to date.[5]

Kinetic and Structural Basis for Efficient and Faithful Bypass of 8-OxoG by Dpo4. Our pre-steady state kinetic studies demonstrate not only that Dpo4 discriminated against the incorporation of incorrect nucleotides, including dAMP opposite 8-oxoG, with a fidelity in the range of 10^{-3} to 10^{-5} (Table 4) but also that the efficiency of correct incorporation both opposite and extending from the lesion is higher than that observed for undamaged DNA (Table 4). To date, only yeast DNA polymerase η has been shown to replicate past 8-oxoG with a similarly high fidelity and efficiency.[13] Our kinetic studies also show that 8-oxoG had almost no effect on maximal nucleotide incorporation rate constants (Table 4), the overall DNA binding affinities (Figure S7 of the Supporting Information), or the productive DNA binding mode (Figure S8 of the Supporting Information), suggesting that Dpo4 likely followed the same kinetic mechanism described for undamaged DNA[32] to bypass and extend from 8-oxoG.

Interestingly, crystallographic studies show that relative to undamaged dG in the Dpo4·DNA·dCTP ternary complex, additional hydrogen bonds form between the LF (R331 and R332) and Finger (S34) domains of Dpo4 and the O8 atom and phosphate group of 8-oxoG (Figure S9A of the Supporting Information),[15,20] which are critical for both the efficiency and the fidelity of 8-oxoG bypass.[22] These extra hydrogen bonds stabilize 8-oxoG in the *anti* conformation but do not exist if 8-oxoG is in the *syn* conformation, leading to both preferential base pairing with dCTP and a 66-fold higher binding affinity (Table 4) of dCTP (K_d = 14 μM) over dATP (K_d = 929 μM). An incorrect dATP is known to form Hoogsteen base pairs with 8-oxoG in the *syn* conformation at the active site of Dpo4.[15] Furthermore, these aforementioned extra hydrogen bonds also stabilized the templating base 8-oxoG slightly more so than dG (Figure S9A,B of the Supporting Information), leading to a 3-fold higher binding affinity of dCTP for the Dpo4·O-21 complex (K_d = 14 μM) than for the Dpo4·C-21 complex [K_d = 49 μM (Table 4)]. Similarly, the embedded 8-oxoG enhanced the binding affinity of the correct dGTP for the Dpo4·O-22 complex by ∼3-fold relative to that for the Dpo4·C-22 complex (Table 4) because of the additional stabilization of O-22 provided by the extra hydrogen bonds formed between Dpo4 and 8-oxoG at the −1 template position (Figure S9C,D of the Supporting Information).[21,44] Thus, these extra hydrogen bonds with 8-oxoG enhanced correct nucleotide binding and incorporation during both the lesion bypass and subsequent extension steps, resulting in the relatively high fidelity of 8-oxoG bypass catalyzed by Dpo4 (Table 4).

Kinetic Basis for the Stalling of Wild-Type PolB1 near an 8-OxoG Site. Many high-fidelity A- and B-family DNA polymerases are able to bypass 8-oxoG but with a fidelity much lower than that observed for undamaged DNA.[9−11,38,45] However, our results demonstrate that wild-type PolB1 completely failed to bypass the lesion (Figure 2B) because of both a reduction in correct nucleotide incorporation efficiency (Table 2) and an increase in the 3′ → 5′ exonuclease activity in the vicinity of the lesion (Table 3 and Figure 5). PolB1 does

dx.doi.org/10.1021/bi300246r | *Biochemistry* 2012, 51, 3485−3496

have an intrinsic ability to incorporate a nucleotide opposite 8-oxoG as observed from assays with its exonuclease-deficient mutant, but the efficiency is decreased by >100-fold compared to that of replication opposite undamaged DNA (Table 2). As detailed in Scheme 1, the greatly increased rate of DNA excision, both at and near the lesion site, exceeds the decreased nucleotide incorporation rate at these sites, effectively preventing the formation of any lesion bypass product. Furthermore, the exonuclease activity is the most rapid in the presence of a terminal 8-oxoG:A mismatch and is also increased with an embedded mismatch at position −1 (Table 3), indicating that wild-type PolB1 can efficiently remove any misincorporation opposite the lesion generated by the polymerase activity of PolB1 or Dpo4. However, our results also indicate that once an 8-oxoG:C base pair has been extended by one nucleotide, the rate of incorporation of a nucleotide into O-23 (Table 1 and Scheme 1) and the rate of excision of the subsequent product O-24 (Table 3 and Scheme 1) return to the levels for undamaged DNA (Table 3), thus allowing PolB1 to switch with Dpo4 and resume replication once the lesion has been bypassed and extended by Dpo4 (Figure 6).

Increased exonuclease activity in response to a DNA lesion has been suggested to play a role in TLS by other DNA polymerases. Elimination of the 3′ → 5′ exonuclease activity has been shown to enhance the ability of *Escherichia coli* polymerases I and II[46,47] as well as human polymerase δ[48] to bypass an abasic site and T4 DNA polymerase to bypass an O^6-methylguanine.[49] However, in each of these cases, unlike the results observed here with PolB1, the lesion did not lead to complete stalling of the wild-type enzyme, and a detailed kinetic basis for the polymerase pausing was not established. Furthermore, the lesions investigated in those studies lead to significant destabilization of the duplex DNA, which may stimulate exonuclease activity,[49] whereas 8-oxoG is not likely to affect the melting temperature of DNA to a similar extent.[4] Consequently, unlike PolB1, the exonuclease activities of T7 DNA polymerase and polymerase δ have little or no effect on their ability to bypass 8-oxoG.[18,48] The 3′ → 5′ exonuclease activity acts to increase the fidelity of a DNA polymerase by promoting the excision of misincorporations that lead to distorted local DNA structure. Thus, the increased exonuclease activity of wild-type PolB1 in the presence of the 8-oxoG lesion may be a result of distorted local DNA geometry rather than a destabilized DNA duplex.

Structural Basis for the Fidelity of PolB1 exo− during 8-OxoG Bypass. Despite the fact that wild-type PolB1 cannot bypass 8-oxoG (Figure 2B), its exonuclease-deficient mutant may utilize a structurally conserved motif to achieve high fidelity when incorporating an incoming dNMP opposite the lesion. The B-family DNA polymerase from bacteriophage RB69 exhibits a relatively high fidelity during 8-oxoG bypass compared to other DNA polymerases.[50] This results from a decreased efficiency of dAMP incorporation because of a steric clash between residues Y567 and G568 and the O8 atom of 8-oxoG when it is in the *syn* conformation.[50,51] Analogous residues play a similar role in 8-oxoG bypass for ϕ29 DNA polymerase and human polymerase γ.[40,52] These tyrosine and glycine residues appear to be highly conserved among A- and B-family DNA polymerases.[53] Consequently, a superimposition of the apo structure of PolB1[54] onto the ternary structure of RB69 DNA polymerase[50] indicates that Y610 and G611 of PolB1 overlay very closely with Y567 and G568 of RB69 DNA polymerase (Figure S10 of the Supporting Information), indicating that these residues serve a similar function in aiding the fidelity of PolB1 exo− during the incorporation of dNMP opposite 8-oxoG. However, because the efficiency of incorporation of dCMP opposite 8-oxoG is 100-fold lower than that of incorporation opposite undamaged dG and 1000-fold lower than that measured for Dpo4 (Tables 2 and 4), the 8-oxoG lesion likely disrupts the active site of PolB1 even when it is in the *anti* conformation.

Role of Kinetics in Polymerase Switching. The complete stalling of wild-type PolB1 at the 8-oxoG site, along with the efficient and faithful bypass of the lesion by Dpo4 is consistent with the model of "polymerase switching" at a lesion site.[41] Our results clearly show that, even in the absence of accessory factor proteins, this switch can occur in vitro in response to an 8-oxoG lesion, as Dpo4 was shown to relieve the pausing of PolB1 at the lesion site (Figure 3 and Figures S1 and S2 of the Supporting Information). PolB1 and Dpo4 may be the only polymerases involved in the switching mechanism in *S. solfataricus*, as the organism's other two DNA polymerases most likely have an activity too low to play a major role in TLS.[27] While our results cannot provide a full picture of the in vivo mechanism of polymerase switching because of the lack of inclusion of the processivity factor PCNA, we are able to propose a hypothetical model for the process based on the kinetic properties of each DNA polymerase elucidated in this work. Wild-type PolB1 will replicate undamaged DNA (Figure 6, complex 1) until it encounters a lesion site, where it will stall (Figure 6, complex 2) as the exonuclease rate (0.098 s^{-1}) is increased to 66-fold higher than the nucleotide incorporation rate (0.0015 s^{-1}) (Scheme 1). During this stalling, PolB1 can transiently dissociate from the replication fork (Figure 6, complex 3). The polymerase·PCNA complex can then rotate to allow Dpo4 to overtake the replication fork and bypass the lesion (Figure 6, complex 4). Dpo4 is also more efficient than PolB1 when extending from the lesion as the rate of extension past the 8-oxoG:C base pair for Dpo4 [0.25 s^{-1} at 200 μM dGTP (Figure S6B of the Supporting Information)] is higher than the rate measured for PolB1 (0.06 s^{-1}) at the same dGTP concentration (Scheme 1). However, the rate of the subsequent nucleotide incorporation catalyzed by Dpo4 [0.18 s^{-1} (Figure S5B of the Supporting Information)] is slightly smaller than the rate (0.21 s^{-1}) measured for PolB1 under the same reaction conditions (Scheme 1). Furthermore, the DNA excision rate and nucleotide incorporation rate of PolB1 are no longer affected by the lesion at this position and beyond (Scheme 1). Thus, once the lesion is bypassed and the lesion bypass product is elongated by at least one nucleotide, Dpo4 can dissociate from the DNA, allowing wild-type PolB1, which replicates undamaged DNA with a fidelity 10^3−10^5-fold higher than that of Dpo4,[33,35] to replace Dpo4 and resume replication (Figure 6, complexes 5 and 6) to maintain the high genomic stability of *S. solfataricus* (see above). The reclaiming of the replication fork by PolB1 may be aided by the 10-fold higher DNA binding affinity of PolB1 compared to that of Dpo4,[32,34] along with Dpo4's slowed conformational dynamics and translocation along the DNA during the extension of the lesion bypass product described in our recent work.[55] Although it is plausible that Dpo4 will be switched off after it extends just one nucleotide post-lesion bypass, the exact position at which PolB1 resumes replication is unclear and requires further investigation. However, our results do suggest that Dpo4 did not overtake the primer−template junction until the lesion was in the templating

position, as the pattern of intermediate product accumulation prior to the lesion site in the presence of both polymerases (Figure 3) mimics that observed for PolB1 alone (Figure 2B). While our results demonstrate that switching can occur in the absence of any other accessory proteins, polymerase switching is thought to be mediated by the processivity factor, proliferating cell nuclear antigen (PCNA), which can act as a tool belt, whereby it is simultaneously bound to both a replicative and a lesion bypass DNA polymerase to facilitate switching between the two enzymes before and after the lesion bypass.[56] Interestingly, *S. solfataricus* PCNA is a heterotrimer, with PolB1 and Dpo4 each known to interact with a different subunit,[57,58] suggesting that this tool belt model for PCNA-mediated polymerase switching may indeed be accurate for *S. solfataricus*. Presumably, PCNA will help prevent the complete dissociation of both Dpo4 and PolB1 from DNA during DNA synthesis. This suggests that competition between PolB1 and Dpo4 for the binding of the primer−template junction near the lesion will be influenced by polymerase kinetics in the presence of PCNA as proposed in Figure 6. Interestingly, it has recently been suggested that PCNA may influence the efficiency and fidelity of lesion bypass for individual polymerases.[23,24] Our results provide a solid foundation for future investigation into the role of PCNA and other replication factors on the mechanism of polymerase switching during TLS.

■ ASSOCIATED CONTENT

Supporting Information

Figures S1−S10. This material is available free of charge via the Internet at http://pubs.acs.org.

■ AUTHOR INFORMATION

Corresponding Author

*Department of Biochemistry, The Ohio State University, Columbus, OH 43210. Telephone: (614) 688-3706. Fax: (614) 292-6773. E-mail: suo.3@osu.edu.

Funding

This work was supported by the National Science Foundation (NSF) Career Award (MCB-0447899) and NSF Grant MCB-0960961 to Z.S.

Notes

The authors declare no competing financial interest.

■ ACKNOWLEDGMENTS

We thank T. Eric Cargal for measuring the k_p and K_d for misincorporation of dAMP into C-21 and Dr. Jason D. Fowler for assistance in preparing figures from gel images.

■ ABBREVIATIONS

8-oxoG, 8-oxo-7,8-dihydro-2′-deoxyguanine; Dpo4, DNA polymerase IV; PAGE, polyacrylamide gel electrophoresis; PCNA, proliferating cell nuclear antigen; PolB1, DNA polymerase B1; PolB1 exo−, exonuclease-deficient PolB1; TLS, translesion DNA synthesis.

■ REFERENCES

(1) Kasai, H. (1997) Analysis of a form of oxidative DNA damage, 8-hydroxy-2′-deoxyguanosine, as a marker of cellular oxidative stress during carcinogenesis. *Mutat. Res. 387*, 147−163.

(2) Cadet, J., Douki, T., Gasparutto, D., and Ravanat, J. L. (2003) Oxidative damage to DNA: Formation, measurement and biochemical features. *Mutat. Res. 531*, 5−23.

(3) Kouchakdjian, M., Bodepudi, V., Shibutani, S., Eisenberg, M., Johnson, F., Grollman, A. P., and Patel, D. J. (1991) NMR structural studies of the ionizing radiation adduct 7-hydro-8-oxodeoxyguanosine (8-oxo-7H-dG) opposite deoxyadenosine in a DNA duplex. 8-Oxo-7H-dG(syn)·dA(anti) alignment at lesion site. *Biochemistry 30*, 1403−1412.

(4) McAuley-Hecht, K. E., Leonard, G. A., Gibson, N. J., Thomson, J. B., Watson, W. P., Hunter, W. N., and Brown, T. (1994) Crystal structure of a DNA duplex containing 8-hydroxydeoxyguanine-adenine base pairs. *Biochemistry 33*, 10266−10270.

(5) Brown, J. A., Duym, W. W., Fowler, J. D., and Suo, Z. (2007) Single-turnover kinetic analysis of the mutagenic potential of 8-oxo-7,8-dihydro-2′-deoxyguanosine during gap-filling synthesis catalyzed by human DNA polymerases λ and β. *J. Mol. Biol. 367*, 1258−1269.

(6) Zhang, Y., Yuan, F., Wu, X., Wang, M., Rechkoblit, O., Taylor, J. S., Geacintov, N. E., and Wang, Z. (2000) Error-free and error-prone lesion bypass by human DNA polymerase κ in vitro. *Nucleic Acids Res. 28*, 4138−4146.

(7) Furge, L. L., and Guengerich, F. P. (1997) Analysis of nucleotide insertion and extension at 8-oxo-7,8-dihydroguanine by replicative T7 polymerase exo- and human immunodeficiency virus-1 reverse transcriptase using steady-state and pre-steady-state kinetics. *Biochemistry 36*, 6475−6487.

(8) Einolf, H. J., Schnetz-Boutaud, N., and Guengerich, F. P. (1998) Steady-state and pre-steady-state kinetic analysis of 8-oxo-7,8-dihydroguanosine triphosphate incorporation and extension by replicative and repair DNA polymerases. *Biochemistry 37*, 13300−13312.

(9) Hsu, G. W., Ober, M., Carell, T., and Beese, L. S. (2004) Error-prone replication of oxidatively damaged DNA by a high-fidelity DNA polymerase. *Nature 431*, 217−221.

(10) Shibutani, S., Takeshita, M., and Grollman, A. P. (1991) Insertion of specific bases during DNA synthesis past the oxidation-damaged base 8-oxodG. *Nature 349*, 431−434.

(11) Lowe, L. G., and Guengerich, F. P. (1996) Steady-state and pre-steady-state kinetic analysis of dNTP insertion opposite 8-oxo-7,8-dihydroguanine by *Escherichia coli* polymerases I exo- and II exo. *Biochemistry 35*, 9840−9849.

(12) Krahn, J. M., Beard, W. A., Miller, H., Grollman, A. P., and Wilson, S. H. (2003) Structure of DNA polymerase β with the mutagenic DNA lesion 8-oxodeoxyguanine reveals structural insights into its coding potential. *Structure 11*, 121−127.

(13) Carlson, K. D., and Washington, M. T. (2005) Mechanism of efficient and accurate nucleotide incorporation opposite 7,8-dihydro-8-oxoguanine by *Saccharomyces cerevisiae* DNA polymerase η. *Mol. Cell. Biol. 25*, 2169−2176.

(14) Rechkoblit, O., Kolbanovskiy, A., Malinina, L., Geacintov, N. E., Broyde, S., and Patel, D. J. (2010) Mechanism of error-free and semitargeted mutagenic bypass of an aromatic amine lesion by Y-family polymerase Dpo4. *Nat. Struct. Mol. Biol. 17*, 379−388.

(15) Zang, H., Irimia, A., Choi, J. Y., Angel, K. C., Loukachevitch, L. V., Egli, M., and Guengerich, F. P. (2006) Efficient and high fidelity incorporation of dCTP opposite 7,8-dihydro-8-oxodeoxyguanosine by *Sulfolobus solfataricus* DNA polymerase Dpo4. *J. Biol. Chem. 281*, 2358−2372.

(16) Picher, A. J., and Blanco, L. (2007) Human DNA polymerase λ is a proficient extender of primer ends paired to 7,8-dihydro-8-oxoguanine. *DNA Repair 6*, 1749−1756.

(17) Beard, W. A., Batra, V. K., and Wilson, S. H. (2010) DNA polymerase structure-based insight on the mutagenic properties of 8-oxoguanine. *Mutat. Res. 703*, 18−23.

(18) Brieba, L. G., Eichman, B. F., Kokoska, R. J., Doublie, S., Kunkel, T. A., and Ellenberger, T. (2004) Structural basis for the dual coding potential of 8-oxoguanosine by a high-fidelity DNA polymerase. *EMBO J. 23*, 3452−3461.

(19) Brieba, L. G., Kokoska, R. J., Bebenek, K., Kunkel, T. A., and Ellenberger, T. (2005) A lysine residue in the fingers subdomain of T7 DNA polymerase modulates the miscoding potential of 8-oxo-7,8-dihydroguanosine. *Structure 13*, 1653−1659.

(20) Rechkoblit, O., Malinina, L., Cheng, Y., Kuryavyi, V., Broyde, S., Geacintov, N. E., and Patel, D. J. (2006) Stepwise translocation of Dpo4 polymerase during error-free bypass of an oxoG lesion. *PLoS Biol. 4*, e11.
(21) Rechkoblit, O., Malinina, L., Cheng, Y., Geacintov, N. E., Broyde, S., and Patel, D. J. (2009) Impact of conformational heterogeneity of OxoG lesions and their pairing partners on bypass fidelity by Y family polymerases. *Structure 17*, 725−736.
(22) Eoff, R. L., Irimia, A., Angel, K. C., Egli, M., and Guengerich, F. P. (2007) Hydrogen bonding of 7,8-dihydro-8-oxodeoxyguanosine with a charged residue in the little finger domain determines miscoding events in *Sulfolobus solfataricus* DNA polymerase Dpo4. *J. Biol. Chem. 282*, 19831−19843.
(23) Maga, G., Villani, G., Crespan, E., Wimmer, U., Ferrari, E., Bertocci, B., and Hubscher, U. (2007) 8-Oxo-guanine bypass by human DNA polymerases in the presence of auxiliary proteins. *Nature 447*, 606−608.
(24) Maga, G., Crespan, E., Wimmer, U., van Loon, B., Amoroso, A., Mondello, C., Belgiovine, C., Ferrari, E., Locatelli, G., Villani, G., and Hubscher, U. (2008) Replication protein A and proliferating cell nuclear antigen coordinate DNA polymerase selection in 8-oxo-guanine repair. *Proc. Natl. Acad. Sci. U.S.A. 105*, 20689−20694.
(25) Bruskov, V. I., Malakhova, L. V., Masalimov, Z. K., and Chernikov, A. V. (2002) Heat-induced formation of reactive oxygen species and 8-oxoguanine, a biomarker of damage to DNA. *Nucleic Acids Res. 30*, 1354−1363.
(26) She, Q., Singh, R. K., Confalonieri, F., Zivanovic, Y., Allard, G., Awayez, M. J., Chan-Weiher, C. C., Clausen, I. G., Curtis, B. A., De Moors, A., Erauso, G., Fletcher, C., Gordon, P. M., Heikamp-de Jong, I., Jeffries, A. C., Kozera, C. J., Medina, N., Peng, X., Thi-Ngoc, H. P., Redder, P., Schenk, M. E., Theriault, C., Tolstrup, N., Charlebois, R. L., Doolittle, W. F., Duguet, M., Gaasterland, T., Garrett, R. A., Ragan, M. A., Sensen, C. W., and Van der Oost, J. (2001) The complete genome of the crenarchaeon *Sulfolobus solfataricus* P2. *Proc. Natl. Acad. Sci. U.S.A. 98*, 7835−7840.
(27) Choi, J. Y., Eoff, R. L., Pence, M. G., Wang, J., Martin, M. V., Kim, E. J., Folkmann, L. M., and Guengerich, F. P. (2011) Roles of the four DNA polymerases of the crenarchaeon *Sulfolobus solfataricus* and accessory proteins in DNA replication. *J. Biol. Chem. 286*, 31180−31193.
(28) Fiala, K. A., Hypes, C. D., and Suo, Z. (2007) Mechanism of abasic lesion bypass catalyzed by a Y-family DNA polymerase. *J. Biol. Chem. 282*, 8188−8198.
(29) Brown, J. A., Newmister, S. A., Fiala, K. A., and Suo, Z. (2008) Mechanism of double-base lesion bypass catalyzed by a Y-family DNA polymerase. *Nucleic Acids Res. 36*, 3867−3878.
(30) Wong, J. H., Brown, J. A., Suo, Z., Blum, P., Nohmi, T., and Ling, H. (2010) Structural insight into dynamic bypass of the major cisplatin-DNA adduct by Y-family polymerase Dpo4. *EMBO J. 29*, 2059−2069.
(31) Sherrer, S. M., Brown, J. A., Pack, L. R., Jasti, V. P., Fowler, J. D., Basu, A. K., and Suo, Z. (2009) Mechanistic studies of the bypass of a bulky single-base lesion catalyzed by a Y-family DNA polymerase. *J. Biol. Chem. 284*, 6379−6388.
(32) Fiala, K. A., and Suo, Z. (2004) Mechanism of DNA polymerization catalyzed by *Sulfolobus solfataricus* P2 DNA polymerase IV. *Biochemistry 43*, 2116−2125.
(33) Fiala, K. A., and Suo, Z. (2004) Pre-steady-state kinetic studies of the fidelity of *Sulfolobus solfataricus* P2 DNA polymerase IV. *Biochemistry 43*, 2106−2115.
(34) Brown, J. A., and Suo, Z. (2009) Elucidating the kinetic mechanism of DNA polymerization catalyzed by *Sulfolobus solfataricus* P2 DNA polymerase B1. *Biochemistry 48*, 7502−7511.
(35) Zhang, L., Brown, J. A., Newmister, S. A., and Suo, Z. (2009) Polymerization fidelity of a replicative DNA polymerase from the hyperthermophilic archaeon *Sulfolobus solfataricus* P2. *Biochemistry 48*, 7492−7501.
(36) Fiala, K. A., Sherrer, S. M., Brown, J. A., and Suo, Z. (2008) Mechanistic consequences of temperature on DNA polymerization catalyzed by a Y-family DNA polymerase. *Nucleic Acids Res. 36*, 1990−2001.
(37) Gruz, P., Shimizu, M., Pisani, F. M., De Felice, M., Kanke, Y., and Nohmi, T. (2003) Processing of DNA lesions by archaeal DNA polymerases from *Sulfolobus solfataricus*. *Nucleic Acids Res. 31*, 4024−4030.
(38) Patro, J. N., Urban, M., and Kuchta, R. D. (2009) Interaction of human DNA polymerase α and DNA polymerase I from *Bacillus stearothermophilus* with hypoxanthine and 8-oxoguanine nucleotides. *Biochemistry 48*, 8271−8278.
(39) Hogg, M., Rudnicki, J., Midkiff, J., Reha-Krantz, L., Doublie, S., and Wallace, S. S. (2010) Kinetics of mismatch formation opposite lesions by the replicative DNA polymerase from bacteriophage RB69. *Biochemistry 49*, 2317−2325.
(40) de Vega, M., and Salas, M. (2007) A highly conserved tyrosine residue of family B DNA polymerases contributes to dictate translesion synthesis past 8-oxo-7,8-dihydro-2′-deoxyguanosine. *Nucleic Acids Res. 35*, 5096−5107.
(41) Cordonnier, A. M., and Fuchs, R. P. (1999) Replication of damaged DNA: Molecular defect in xeroderma pigmentosum variant cells. *Mutat. Res. 435*, 111−119.
(42) Fiala, K. A., Brown, J. A., Ling, H., Kshetry, A. K., Zhang, J., Taylor, J. S., Yang, W., and Suo, Z. (2007) Mechanism of Template-independent Nucleotide Incorporation Catalyzed by a Template-dependent DNA Polymerase. *J. Mol. Biol. 365*, 590−602.
(43) Grogan, D. W., Carver, G. T., and Drake, J. W. (2001) Genetic fidelity under harsh conditions: Analysis of spontaneous mutation in the thermoacidophilic archaeon *Sulfolobus acidocaldarius*. *Proc. Natl. Acad. Sci. U.S.A. 98*, 7928−7933.
(44) Vaisman, A., Ling, H., Woodgate, R., and Yang, W. (2005) Fidelity of Dpo4: Effect of metal ions, nucleotide selection and pyrophosphorolysis. *EMBO J. 24*, 2957−2967.
(45) Einolf, H. J., and Guengerich, F. P. (2001) Fidelity of nucleotide insertion at 8-oxo-7,8-dihydroguanine by mammalian DNA polymerase δ. Steady-state and pre-steady-state kinetic analysis. *J. Biol. Chem. 276*, 3764−3771.
(46) Paz-Elizur, T., Takeshita, M., and Livneh, Z. (1997) Mechanism of bypass synthesis through an abasic site analog by DNA polymerase I. *Biochemistry 36*, 1766−1773.
(47) Paz-Elizur, T., Takeshita, M., Goodman, M., O'Donnell, M., and Livneh, Z. (1996) Mechanism of translesion DNA synthesis by DNA polymerase II. Comparison to DNA polymerases I and III core. *J. Biol. Chem. 271*, 24662−24669.
(48) Fazlieva, R., Spittle, C. S., Morrissey, D., Hayashi, H., Yan, H., and Matsumoto, Y. (2009) Proofreading exonuclease activity of human DNA polymerase δ and its effects on lesion-bypass DNA synthesis. *Nucleic Acids Res. 37*, 2854−2866.
(49) Khare, V., and Eckert, K. A. (2001) The 3′ → 5′ exonuclease of T4 DNA polymerase removes premutagenic alkyl mispairs and contributes to futile cycling at O6-methylguanine lesions. *J. Biol. Chem. 276*, 24286−24292.
(50) Freisinger, E., Grollman, A. P., Miller, H., and Kisker, C. (2004) Lesion (in)tolerance reveals insights into DNA replication fidelity. *EMBO J. 23*, 1494−1505.
(51) Beckman, J., Wang, M., Blaha, G., Wang, J., and Konigsberg, W. H. (2010) Substitution of Ala for Tyr567 in RB69 DNA polymerase allows dAMP to be inserted opposite 7,8-dihydro-8-oxoguanine. *Biochemistry 49*, 4116−4125.
(52) Graziewicz, M. A., Bienstock, R. J., and Copeland, W. C. (2007) The DNA polymerase γ Y955C disease variant associated with PEO and parkinsonism mediates the incorporation and translesion synthesis opposite 7,8-dihydro-8-oxo-2′-deoxyguanosine. *Hum. Mol. Genet. 16*, 2729−2739.
(53) Blanco, L., Bernad, A., Blasco, M. A., and Salas, M. (1991) A general structure for DNA-dependent DNA polymerases. *Gene 100*, 27−38.
(54) Savino, C., Federici, L., Johnson, K. A., Vallone, B., Nastopoulos, V., Rossi, M., Pisani, F. M., and Tsernoglou, D. (2004) Insights into

DNA replication: the crystal structure of DNA polymerase B1 from the archaeon *Sulfolobus solfataricus*. *Structure 12*, 2001−2008.
(55) Maxwell, B. A., Xu, C., and Suo, Z. (2012) A DNA Lesion Alters the Global Conformational Dynamics of a Y-Family DNA Polymerase during Catalysis. *J. Biol. Chem. 287*, 13040−13047.
(56) Pages, V., and Fuchs, R. P. (2002) How DNA lesions are turned into mutations within cells? *Oncogene 21*, 8957−8966.
(57) Dionne, I., Nookala, R. K., Jackson, S. P., Doherty, A. J., and Bell, S. D. (2003) A heterotrimeric PCNA in the hyperthermophilic archaeon *Sulfolobus solfataricus*. *Mol. Cell 11*, 275−282.
(58) Xing, G., Kirouac, K., Shin, Y. J., Bell, S. D., and Ling, H. (2009) Structural insight into recruitment of translesion DNA polymerase Dpo4 to sliding clamp PCNA. *Mol. Microbiol. 71*, 678−691.